Effects of Fluid Axial Dispersion and Particles' Packing Inhomogeneity at Supercritical Fluid Extraction

Arthur A. Salamatin*
Mail address: 420008, Russia, Kazan, 35 Kremlyovskaya str., room 503
E-mail: Arthouse131@rambler.ru; Fax: +7 (843) 292-72-79

ABSTRACT

The error of neglecting fluid flow dispersion effects and influence of inhomogeneous polydisperse particle ensemble distribution variable along the vessel are examined in the framework of the shrinking core model. Computational experiments, performed on the basis of different correlations for axial dispersion coefficient, available from publications, show that the impact of the fluid flow dispersion on the Overall Extraction Curve (OEC) prediction does not exceed 10%. Similar conclusions are deduced from modelling SFE process in packed beds with different particle packing patterns, i.e. homogeneous pack, locally monodisperse stratified (LMS) bed with particle size decreasing along the vessel, and inversely distributed (ILMS) pack. Earlier, LMS and ILMS packs were proven to respectively provide the maximum and minimum extraction degrees. This fact allows the estimation of possible deviations in extraction rates for different types of particles packing to be less than 7% for typical laboratory-scale conditions. Nevertheless, while the OEC divergence is insignificant, the outlet concentration may vary up to 200%.

INTRODUCTION

Supercritical Fluid Extraction (SFE) is a novel technological approach to extract natural compounds from plant materials. It uses solvents (e.g. CO_2) at supercritical conditions which are environmentally friendly, and non-toxic. The new technology is widely used in pharmaceutical production, and food and biofuel industry [1].

Elaborate models facilitate the understanding of the internal and external fundamental processes which govern SFE [2-4]. Inside the particles, two components, cell membranes and cell walls, of plant buildup which potentially control the internal mass transfer, can be distinguished. Accordingly, two limiting approaches – Shrinking Core (SC) [5] and Broken-and-Intact Cells (BIC) [4] models – have been developed and successfully used in data interpretation [4-6]. Moreover, the extended polydisperse SC-model [6] and BIC approach equally provide the same accuracy.

The porous and polydisperse, e.g. bidisperse [6], nature of the packed bed leads to several effects theoretically and numerically investigated here. Non-uniform fluid (solvent) flow in the bed voids leads to Taylor axial dispersion of solute coupled with its molecular diffusion. Both mass-transport mechanisms are traditionally described in terms of convective diffusion (axial dispersion) coefficient D_{ax}. On microscale this coefficient is generally determined by characteristic pore space size. At the same time, the presence of small, dust (~ 50 μm) particles producing solute much faster than the bigger (~ 500 μm) particle fraction decreases the characteristic spatial scale of solute concentration change, and, therefore makes dispersion more pronounced. The macroscale master-equation of convective solute-mass transfer in the packed bed is traditionally formulated in the one-dimensional approximation along the vessel with time-derivative and dispersion terms generally taken into account [7]. The uniform velocity distribution over the vessel cross-section is assumed.

Usually, the polydisperse ground raw material is considered to be well-mixed before packing and uniformly distributed inside the vessel. As a consequence, the macroscale mass transfer equation is traditionally restricted to homogeneous and isotropic packed beds [2-10]. Yet, the polydisperse nature of the ground plant material can result either in accidental or controllable axial inhomogeneity of particles packing [8]. The packed beds, non-uniformly distributed along the vessel, under certain special conditions [9] can provide an essential decrease in extraction time, therefore affecting SFE kinetics. However, to the author's knowledge, no publications have been devoted to this study so far.

The present study is focused on the impact of axial dispersion and influence of packed bed inhomogeneity as related to extraction characteristics, namely, Overall Extraction Curve (OEC) and solute concentration in the pore phase. Various theoretical [10, 11] and empirical [12-14] correlations for dispersion coefficient D_{ax} and typical laboratory-scale extraction conditions are considered. Locally bidisperse and monodisperse fractional compositions in packed beds have been examined. The axial inhomogeniety of particles packing has been simulated for Locally Monodisperse Stratified (LMS), Inverse LMS (ILMS) and Uniformly Distributed (UD) packs [8, 9].

MODEL FORMULATION

Basic mass-balance equations. Let us introduce the time t of the SFE process, axial coordinate z varying from 0 at the vessel's inlet to H at the top, superficial (filtration) velocity v, packed bed porosity e, and convective diffusion (axial dispersion) coefficient D_{ax}. Recent analysis of representative SFE kinetic data [6], based on the bidisperse approximation of fractional composition of the packed beds, showed that even sub-division of polydisperse particle ensemble in two fractions may be quite sufficient to simulate relatively short-term laboratory experiments. With f_i , $i = 1..n$ being the volume fraction of the i-th particles fraction in the ground material, loaded into the extractor, particles are considered as spheres of radius a. In the bidisperse approach [6] dust-fraction represents the so-called free solute [2, 4], and the fraction of bigger particles controls the extraction rate at the final extraction step, with negligibly small outlet concentration.

The mass balance master-equation in the pore phase could be written in terms of the solute mass concentration $0 \le c \le 1$, normalized by the solute saturation concentration θ_* in the solvent, as follows

$$e\frac{\partial c}{\partial t} + v\frac{\partial c}{\partial z} - D_{ax}\frac{\partial^2 c}{\partial z^2} = 3(1-e)\sum_{i=1}^{n}\frac{q(a_i,z,t)}{a_i}p_i(z), \quad \sum_{i=1}^{n} p_i \equiv 1, \quad \int_0^H p_i dz = Hf_i . \tag{1}$$

The function $p_i(z)$ shows which cross-sectional volume fraction the i-th fraction occupies in cross-section z, and $p_i = f_i$ for UD packs. Other values correspond to various packing patterns, e.g. LMS and ILMS, which are discussed later in the corresponding section. The solute flux q from the particle surface per its unit area is determined by the microscale diffusion model and mass transfer resistance across the fluid boundary layer around the particle.

Hereinafter, we employ the SC approach, generally valid for ground oilseeds, [5, 10] to formulate the microscale model. This implies the existence of the moving oil extraction front $0 \le R(t, a) \le a$ inside every particle, separating its internal oil containing core from the outer exhausted transport zone. The core shrinks in the course of extraction, and particle becomes fully depleted at $R = 0$. The SC description is applicable in case of relatively high

initial oil content $\theta_0 \gg \theta_*$, and assumes significantly lower mass transfer resistance of cell membranes in comparison with that of the transport channels (cell walls). Finally, for each particle, the solute transport model takes the form of the Koshi problem with respect to the shrinking core radius

$$-\frac{\theta_0}{\theta_*}\frac{\partial}{\partial t}\left(\frac{R}{a}\right)^3 = 3q/a, \quad q = \frac{D_{\text{eff}}}{a}\frac{R/a}{1-R/a}(1-c), \quad R\big|_{t=0} = a, \tag{2}$$

where D_{eff} is the apparent internal solute diffusion coefficient.

Due to high oil diffusivity in solvent phase outside the particles, the external mass transfer resistance between particle surface and solvent is neglected [10].

Scale analysis. The characteristic spatial and temporal scales of the SFE process can be defined [10] as

$$z_{\text{sc}}\left(a_{\text{sc}}\right) = \frac{v a_{\text{sc}}^2}{6D_{\text{eff}}(1-e)}, \quad t_{\text{sc}}\left(a_{\text{sc}}\right) = \frac{\theta_0}{\theta_*}\frac{a_{\text{sc}}^2}{6D_{\text{eff}}} \tag{3}$$

both for mono- and bidisperse packed beds, with corresponding choice of a_{sc}.

For monodisperse beds ($n = 1$) a_{sc} is equal to a_1, and z_{sc} is the length of the so-called extraction zone [10, 15]. By definition, particles in this part of the vessel are currently in the progress of extraction, and $0 < R(t, a_1) < a_1$. The extraction zone initially develops in the vicinity of the vessel inlet, and then moves towards the vessel outlet. Behind this zone, upstream the solvent flow, all particles are exhausted, $R = 0$ and $c = 0$, while in front of the extraction zone, in downstream direction they remain full, $R = a_1$ and $c = 1$. Similar to z_{sc}, being the width of the extraction zone where c increases from 0 to 1, the time scale t_{sc} is the duration of the particle full extraction at typical particle size a_{sc}. Thus, t_{sc} is the characteristic time scale of concentration decrease from 1 to 0 at any given cross-section.

More complicated situation is met in case of bidisperse bed [6], when particle ensemble consists of two fractions of essentially different particle size (representative scales), $a_1 / a_2 \sim 0.1$. The corresponding particle full extraction times $t_{\text{sc}}(a_1)$ and $t_{\text{sc}}(a_2)$ differ by two orders in magnitude. The total length $z_{\text{sc}}(a_2)$ of the extraction zone is determined by the second fraction of bigger particles with $0 < R(a_2) < a_2$. However, since $q_1 \gg q_2$, a shorter subzone $z_{\text{sc}}(a_1)$ of a_1 particles incomplete extraction ($0 < R(a_1) < a_1$) should be distinguished with much higher concentration gradients as compared to those in the other extraction zone sub-region controlled by extraction of the bigger particles where $R(a_1) = 0$.

So, the bidisperse packed bed is characterized by two pairs of time-space scales, defined by particle sizes a_1 and a_2 respectively. We are restricted here by typically short-term extraction processes, when the experiment duration is on the same order as initial solubility-controlled extraction step duration. Thus, the pair of process characteristic scales is determined by the smallest particle size, a_1, in the bed for either mono- or bidisperse beds.

SFE model in dimensionless form. Following [6, 8-10], Eqs. (1) and (2) can be rewritten in terms of dimensionless characteristics as

$$\delta_t \frac{\partial c}{\partial \tau} + \frac{\partial c}{\partial \zeta} - \delta_{\text{ax}} \frac{\partial^2 c}{\partial \zeta^2} = \sum_{i=1}^{n} \frac{\partial s_i}{\partial \tau} p_i, \quad \delta_t = \frac{e z_{\text{sc}}}{v t_{\text{sc}}}, \quad \delta_{\text{ax}} = \frac{D_{\text{ax}}}{v z_{\text{sc}}}, \tag{4}$$

$$\frac{\partial s_i}{\partial \tau} = \frac{\lambda(s_i)}{\xi_i^2}(1-c), \quad s_i = 1-\left(\frac{R_i}{a_i}\right)^3, \quad \lambda(s) = \max\left\{0, \quad \frac{0.5(1-s)^{1/3}}{1-(1-s)^{1/3}}\right\}. \tag{5}$$

Here ζ, τ, and ξ_i are the scaled analogues of axial coordinate $z = \zeta z_{sc}$, time $t = \tau t_{sc}$, and particle radii $a_i = \xi_i a_{sc}$.

Due to the scales, chosen as typical, all the derivatives in Eq. (4) are on the order of $O(1)$, and the magnitude of every term in Eq. (4) is determined by the δ-factors. In particular case of scales (3) at $a_{sc} = a_1$, dimensionless δ-complexes are given by

$$\delta_t = \frac{e}{1-e}\frac{\theta_*}{\theta_0}, \quad \delta_{ax} = 6(1-e)\frac{D_{eff} D_{ax}(a_n)}{a_1^2 v^2}.$$

Obviously, δ_t is small under assumption $\theta_* \ll \theta_0$, and the first term on the left hand side in Eq. (4) can be neglected. SC-model constraining [6] confirmed that the SC-approach and the quasy-stationary approximation at the macroscale level are valid for $\delta_t < 0.05$.

The similarity criterion, inverse dispersion number, δ_{ax}^{-1} has the meaning of Pecklet number with appropriate choice of characteristic spatial scale. Physical features of the process under consideration, such as limited solute solubility in the solvent and finite particle full extraction time, result in characteristic spatial scale of concentration gradient in the pore phase equal to the extraction zone width, instead of vessel height.

Neglecting by time-derivative term, the macroscale mass-balance is written in the form of quasi-stationary convective approximation accounting for axial dispersion and homogeneous particle distribution in the vessel

$$\frac{\partial c}{\partial \zeta} - \delta_{ax}\frac{\partial^2 c}{\partial \zeta^2} = \sum_{i=1}^{n}\frac{\partial s_i}{\partial \tau} p_i \,. \tag{6}$$

Conventionally, Danckwert's boundary conditions known as the open-close vessel approximation are formulated for solute concentration c in the pore phase to analyze [3, 7] axial dispersion. They are the solute flux continuity conditions imposed at the inlet and outlet of the vessel

$$c(0,\tau) - \delta_{ax}\frac{\partial c}{\partial \zeta}(0,\tau) = 0\,, \tag{7a}$$

$$-\delta_{ax}\frac{\partial c}{\partial \zeta}(\eta_1,\tau) = 0\,, \tag{7b}$$

where $\eta_1 = H / z_{sc}(a_1)$ is the normalized vessel height, i.e. dimensionless outlet coordinate, which can be considered as a similarity criterion related to axial dispersion impact. The value $\eta_1 - 1$ is equal to the ratio of packed bed full extraction time to the individual particle extraction time $t_{sc}(a_1)$.

The simplified convective mass transfer equation [6, 8] neglecting dispersion effects is formally obtained from Eq. (6) at $D_{ax} = 0$ ($\delta_{ax} = 0$)

$$\frac{\partial c}{\partial \zeta} = \sum_{i=1}^{n} \frac{\partial s_i}{\partial \tau} p_i \qquad (8)$$

with the reduced inlet condition (7a) becomes

$c(0,\tau) = 0$.

Packed bed axial inhomogeneity. To estimate the impact of the packed bed axial inhomogeneity on the OEC and outlet concentration, one can consider a limiting bidisperse approximation of the packed bed, at $n = 2$. The upper and lower bounds for the extraction characteristics correspond [8] to LMS and ILMS packs, respectively. The following values of p_1 describe these two cases

$$p_1^{\mathrm{LMS}}(\zeta) = \begin{cases} 0, & 0 \le \zeta < f_2\eta, \\ 1, & f_2\eta \le \zeta \le \eta, \end{cases} \qquad p_1^{\mathrm{OLMS}}(\zeta) = \begin{cases} 1, & 0 \le \zeta < f_1\eta, \\ 0, & f_1\eta \le \zeta \le \eta. \end{cases}$$

Thus, it is assumed that the packed bed is a sequence of two monodisperse and homogeneous sub-beds of particles either of size a_1 or a_2, and the LMS and ILMS packings of the bidisperse ground raw material differ only by the order of the particle fractions in the vessel.

RESULTS

Correlations for axial dispersion coefficient. Conventionally, semi-empirical correlations for D_{ax} assume that its ratio to molecular diffusion coefficient D_{12} depends on either Pecklet number $\mathrm{Pe_m} = 2a_n v / D_{12}$, or Reynolds number Re, or both, $\mathrm{Pe_m}$ and Re. The first group is commonly used for modelling dispersion effects in chemical engineering, particularly, in SFE studies [3, 7, 10-14]. Based on these correlations, one can estimate δ_{ax}-values in Eqs. (4)-(7) typical for extraction conditions. With this in mind, for effective diffusion coefficient $D_{\mathrm{eff}} \equiv \varepsilon D_{12}$ on the order of 10^{-12} $\mathrm{m^2 s^{-1}}$ [6] consistent with molecular diffusion coefficient $D_{12} \sim 10^{-9}$–10^{-8} $\mathrm{m^2 s^{-1}}$ and $\varepsilon \sim 10^{-4}$–10^{-3}, at typical bigger fraction particle size $a_n \sim 100$ –1000 μm, the calculated curves of δ_{ax} as a function of v are presented in Fig 1 for monodisperse and bidisperse packed beds.

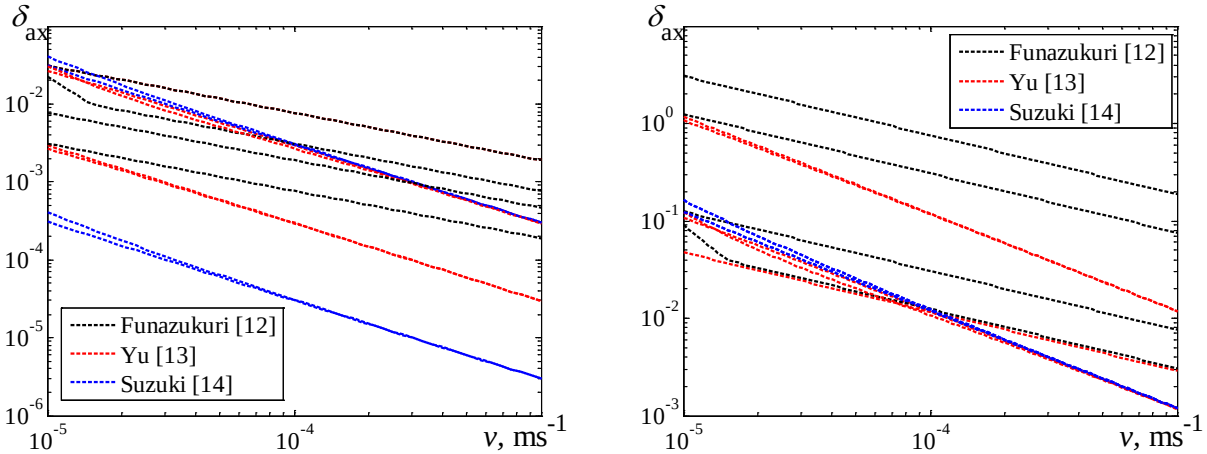

Figure 1: Upper and lower bounds of δ_{ax}-values versus v for monodisperse (left), and bidisperse (right), $a_1 = 50$ μm, packed beds at limiting variations of a_n and D_{12} (see text)

As expected, δ_{ax} decreases with v not exceeding 0.04 for monodisperse beds and being less than 3 for bidisperse packs for $v > 10^{-5}$ ms^{-1}. Available theoretical estimates [10, 11] confirm this conclusion, predicting the δ_{ax}-values within the same range or even smaller.

Monodisperse packed beds. Packed beds, considered in monodisperse approximation, are characterized only by two similarity criteria, δ_{ax} and $\eta = \eta_1$. It is possible to systematically investigate the impact of convective diffusion on the principal outlet characteristics, i.e. OEC and concentration. With this aim, Eqs. (5)-(7) have been numerically solved at different η. Two $\{Y, c\}$-sets simulated at $\delta_{ax} = 0.04$ and 0 (hereinafter designated by respective superscripts "ax" and "0") are presented and intercompared in Fig 2 for representative values of $\eta^{-1} = \{0.25; 0.81; 4; 9; 25; 81\}$ Their relative deviations $E[Y]$ and $E[c]$ have been estimated as $E[X] = |1 - X^{ax}/X^0|$ at X substituted by Y or c.

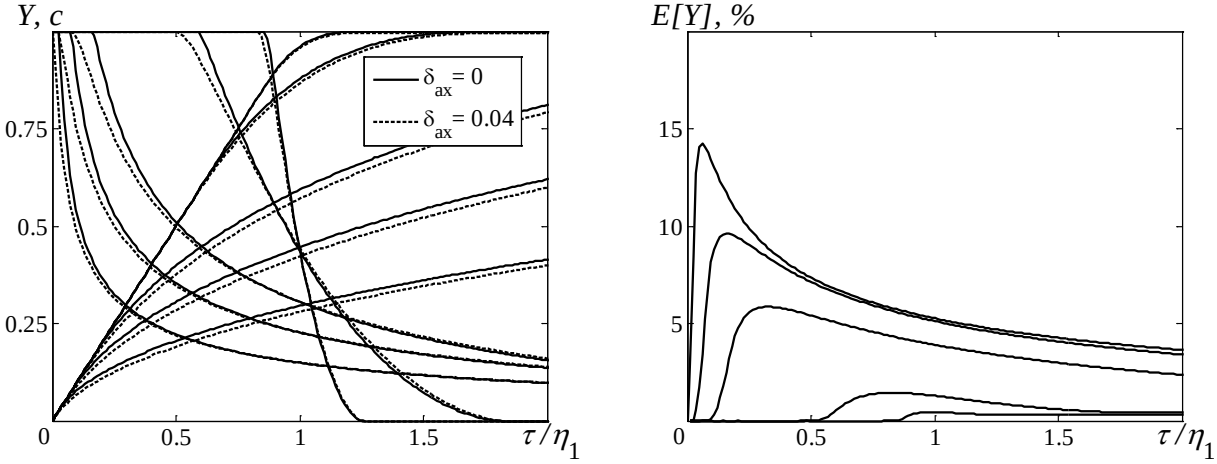

Figure 2: (left) OECs and outlet cross-section concentrations, and (right) relative difference $E[Y]$ between OECs for monodisperse packed beds. Lines correspond to different η-values (see text)

Both Y- and c-curves in Fig. 2 (left) are very similar and closely agree with each other at different values of axial dispersion numbers $\delta_{ax} = 0.04$ and $\delta_{ax} = 0$. The more precise deviation measure $E[Y]$ is shown in Fig. 2 (right). Its maximum decreases with t_{CER}, or, equally, with η. While the $E[Y]$-curves are smooth, the $E[c]$ behavior is rather irregular (not presented here), and amplitudes of its short-term rises are one or two orders higher than those of OEC. As presumed by Fiori et. al. [7], the maximum of $E[Y]$ is reached when the extraction zone approaches the vessel outlet. Nevertheless, the average difference remains less than 5% and is negligible.

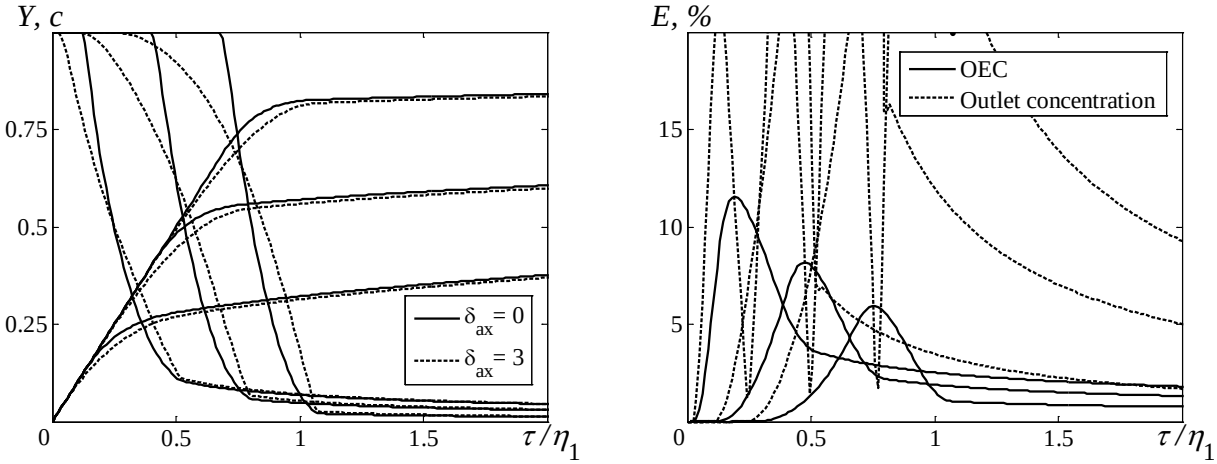

Figure 3: (left) OECs and outlet cross-section concentrations, and (right) relative difference between OECs and outlet cross-section concentrations. Lines correspond to different f_1-values (see text)

Bidisperse packed beds. More complex, bidisperse, packed beds are characterized by four similarity numbers: δ_{ax}, $\eta_i \equiv \eta(a_i)$, $n = 1, 2$, and f_1. In spite of the fact that the maximum value of δ_{ax} for bidisperse beds is two orders of magnitude greater, the influence of axial fluid dispersion on the SFE kinetics is even less prominent as compared to monodisperse beds. Similar $E[Y]$-behaviour can be observed in Fig. 3 where $E[Y]$-maximum decreases with t_{CER}. However, for bidisperse packed beds $t_{CER} \sim f_1$ [6], and only slightly depends on η_i as illustrated by Fig. 3 for a representative set of $f_1 = \{0.2; 0.5; 0.8\}$.

Packed bed axial inhomogeneity. Once the axial dispersion effects are neglected ($\delta_{ax} = 0$), the SFE characteristics are defined by three similarity criteria: fractional composition, f_1, and relative particle extraction time η_i, $i = 1, 2$. In laboratory experiments, $2 < \eta_1 < 10$, while $10^{-4} < \eta_2 < 1$, depending on the grinding degree. A typical case of $H = 15$ cm, $D_{eff} = 10^{-12}$ m^{2}s^{-1}, $v = 10^{-4}$ ms^{-1}, $a_1 = 33$ μm, $a_2 = 735$ μm, i.e. at $\eta_1 = 5$ and $\eta_2 = 10^{-2}$, with $f_1 = \{0.2; 0.5; 0.8\}$ is presented in Fig. 4. The deviation between the two limiting types of packing is calculated as $E_p = |(Y^{LMS} - Y^{OLMS}) / Y^{UD}|$.

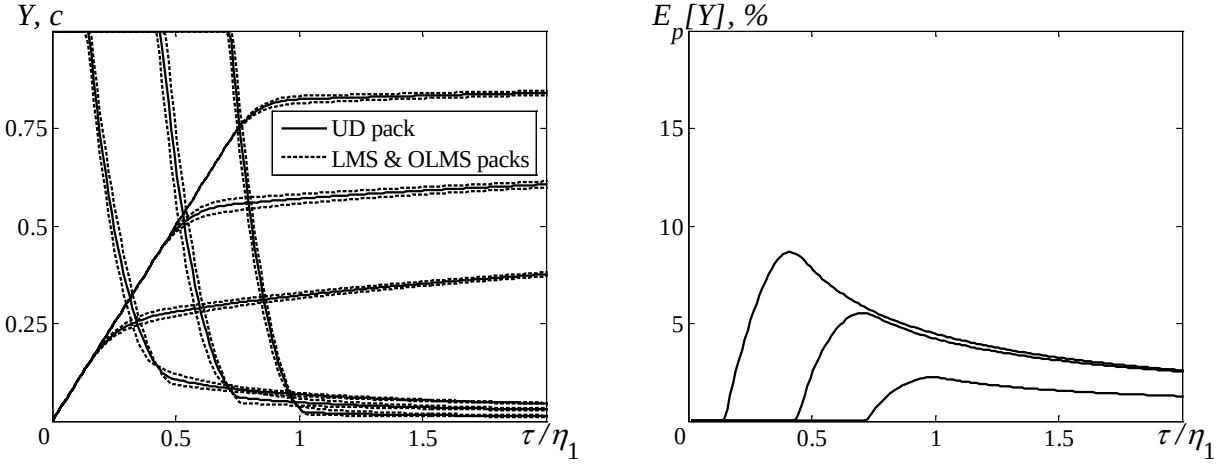

Figure 4: (left) relative difference between OECs and outlet cross-section concentrations, and (right) OECs and outlet cross-section concentrations for three types of packed bed anisotropy. Lines correspond to different f_1-values (see text)

$E_p[Y]$-curves, Fig 4 (right), are similar to those of $E[Y]$-deviations in Figs. 2 and 3 (right) both in their magnitude and general behaviour. The maximum of $E_p[Y]$ and its average also decrease with t_{CER}.

CONCLUSION

The fluid axial dispersion and possible inhomogeneity of packing polydisperse particle ensemble along the vessel at SFE do not essentially affect the overall oil concentrations and production rates with maximum variations of 5-10 % in quasi-stationary approximation at low cumulative inertia of the bed, $\delta_t \to 0$. Thus, one may believe that other microscale models, different from employed SC approach, as well as non-stationary macroscale SFE description will not reveal any new, unexpected effects in Eq. (4) in comparison with its simplified analogues (6) and (8). Furthermore, axial inhomogeneity of packed beds is actually even less pronounced than in the considered limiting LMS and ILMS cases since the dust fraction can hardly be efficiently separated from the main fraction of ground material. Accordingly, fluid axial dispersion renders a similar effect on the overall extraction curve as bed polydispersity, and, for example, in bidisperse packed beds the fluid dispersion could be imitated by a

slightly modified apparent radius a_1 of the dust fraction. The significance of both examined effects diminishes with the constant-extraction-rate time t_{CER}.

Importantly, the t_{CER}-parameter is affected mostly by the free-oil content [6] of the packed bed, i.e. by the volume fraction f_1 of smaller particles in the case of bidisperse particle ensemble. This is a typical practical situation [6], and the corresponding SC-model extension [4, 6], which explicitly accounts for the free-oil trapped by the dust particle fraction, becomes a robust tool in SFE simulations in parallel with the BIC model.

ACKNOWLEGMENTS

This study was supported by the Russian Foundation for Basic Research and by the Academy of Science of Republic of Tatarstan through the grant No. 15-41-02542 r_povolzhe_a, and grant No. 16-31-00007 mol_a.

REFERENCES

[1] Brunner, G., Gas Extraction, Springer, New York, NY, **1994**.

[2] Oliveira, E.L.G., Silvestre, A.J.D., Silva, C.M., Chemical Engineering Research and Design, Vol. 89, **2011**, p. 1104

[3] Sovova, H., Stateva, R.P., Reviews in Chemical Engineering, Vol. 27, **2011**, p. 79

[4] Sovova, H., Chemical Engineering Science, Vol. 49, **1994**, p. 409

[5] Goto, M., Roy, B.C., Hirose, T., The Journal of Supercritical Fluids, Vol. 9, **1996**, p. 128

[6] Egorov, A.G., Salamatin, A.A., Chemical Engineering and Technology, Vol. 38, **2015**, p. 1203

[7] Fiori, L., Calcagno, D., Costa, P., The Journal of Supercritical Fluids, Vol. 41, **2007**, p. 31

[8] Salamatin, A.A., Egorov, A.G., The Journal of Supercritical Fluids, Vol. 105, **2015**, p. 35

[9] Egorov, A.G., Salamatin, A.A., Russian Mathematics, Vol. 59, **2015**, p. 48

[10] Maksudov, R.N., Egorov, A.G., Mazo, A.B., Alyaev, V.A., Abdullin, I.Sh., Sverhkriticheskie Fluidy: Teoriya i Praktika / Supercritical Fluids: Theory and Practice, Vol. 3, **2008**, p. 20 [in Russian]

[11] Kheifets, L.I., Neimark, A.V., Multiphase Processes in Porous Media, Nauka, Khimia, Moscow, **1982** [in Russian]

[12] Funazukuri, T., Kong, Ch., Kagei, S. The Journal of Supercritical Fluids. Vol. 13, **1998**, p. 169

[13] Yu, D., Jackson, K., Harmon, T.C. Chemical Engineering Science. Vol. 54, **1999**, p. 357

[14] Suzuki, M., Smith, J.M. The Chemical Engineering Journal. Vol. 3, **1972**, p. 256

[15] Egorov, A.G., Mazo, A.B., Maksudov, R.N., Theoretical Foundations of Chemical Engineering. Vol. 44, **2010**, p. 642